Hindawi
Mathematical Problems in Engineering
Volume 2022, Article ID 1543625, 7 pages
https://doi.org/10.1155/2022/1543625

Research Article

Rotating Machinery Fault Diagnosis Based on Adaptive Vibration Signal Processing under Safety Environment Conditions

Jingran Zhen

School of Mechanical and Electrical Vehicle Engineering, Zhengzhou Institute of Technology, Henan, Zhengzhou 450044, China

Correspondence should be addressed to Jingran Zhen; 20071051@zzut.edu.cn

Received 14 March 2022; Accepted 21 April 2022; Published 20 May 2022

Academic Editor: Fuli Zhou

At present, the degree of industrialization in China is deepening, and various types of production equipment appear. However, during the startup and operation of mechanical equipment, fracture and wear will occur due to various factors. Therefore, once the mechanical equipment fails, it must be diagnosed as soon as possible to avoid serious economic losses and casualties. Rotating machinery is an important power device, so it is necessary to regularly detect and monitor equipment signals to avoid the consequences of wrong control methods. In this study, the fault diagnosis of rotating machine based on adaptive vibration signal processing is studied under the safe environmental conditions. The fault diagnosis process of rotating machinery is to first collect vibration signals, then process signal noise reduction, and then extract fault characteristic signals to further identify and classify fault status and diagnose fault degree. This study briefly introduces several rotating machinery vibration signal processing methods and identifies the fault state of the rotating machine based on the high-order cumulant. By building a DDS fault diagnosis test bench, the chaotic particle swarm parameter optimization algorithm is used to calculate the accurate stochastic resonance parameters. After noise processing, the high-frequency part is significantly reduced. The results show that, after stochastic resonance wavelet decomposition and denoising processing, the number of intrinsic functions can be significantly reduced, the fault frequency can be increased, the high-frequency noise can be reduced, and the fault analysis accuracy can be improved. We identify the fault state of rotating machinery based on the high-order cumulant, train the four states of the bearing, and compare the four types of faults, no fault, inner ring fault, rolling element fault, and outer ring fault through the comparison of the actual test set and the predicted test set. It is concluded that the rotating machinery fault belongs to the rolling element fault and the identification accuracy rate is 95%. Finally, based on the LMD morphological filtering, the rotating machinery fault diagnosis is carried out, and the feature extraction is carried out based on the LMD algorithm to decompose the bearing fault signal. Finally, the result after the morphological filtering and LMD decomposition and extraction can avoid noise interference.

1. Introduction

In recent years, modern industry and modern technology have shown a rapid development trend. In the future, rotating machinery will develop towards high-speed, integrated, and automated trends, and the level of intelligence is increasing, the structure is more complex, and the components are closely connected [1, 2]. In case of failure, it will form a chain reaction, seriously damage the normal operation of the equipment, cause incalculable economic losses, and even cause casualties [3]. There have been many casualties caused by this factor at home and abroad.

Rotating machinery is a common power plant, mainly used in ships, power generation, aerospace, and other fields, and has a certain role in promoting the national economy in China [4, 5]. Mechanical fault diagnosis is based on a comprehensive grasp of the actual operating status of equipment, to determine whether equipment is partially or overall faulty and to find the fault and the causes of the fault in advance [6]. The main measure of fault diagnosis is to extract fault features. Since the mechanical equipment system is complex and requires a large number of components, the signal obtained by the signal measurement and acquisition system is the effect of the interaction of all components, and the transmission state of the signal in the channel makes each component [7, 8]. The degree of mixing of signal components is increased. Therefore, when diagnosing faults, it is necessary to first process the mixed signals

formed in the system to obtain signal information characteristics and then further diagnose the faults of large or complex mechanical equipment [9–11].

The economic benefits formed by fault diagnosis technology after years of development are huge. Countries around the world have recognized the advantages of rotating machinery fault diagnosis and invested a lot of manpower and funds to study this field [12, 13]. By using the advanced level of diagnostic technology, the United States is at the forefront of the world. The monitoring products developed by some companies in the United States, as the current frontier of diagnostic technology, have multiple monitoring functions and powerful diagnostic functions, which can be used in chemical, military, and other fields [14, 15]. Chinese experts use local mean decomposition (LMD) algorithm combined with LabVIEW software to analyze bearing experimental signals, and some other experts use LMD and order tracking analysis method to diagnose rotating bearing faults under variable speed conditions [16, 17].

This study analyzes the fault diagnosis process of rotating machinery, uses sensors to collect vibration signals, performs noise reduction processing based on stochastic resonance theoretical model, identifies rotating machinery fault status based on high-order cumulants, and uses LMD morphological filtering to diagnose rotating machinery faults. The research shows that the most important part in the fault diagnosis of rotating machinery is to extract the fault features. Effectively dealing with the faults of the mechanical equipment is convenient for the reliable and safe operation of the equipment.

2. Materials and Methods

2.1. Rotating Machinery Fault Diagnosis Process. More than 70% of the faults in rotating machinery and equipment are shaft and bearing faults. Bearing faults include inner ring faults, rotor faults, and outer ring faults. The main factors leading to the failure are unreasonable assembly, long-term overload operation, fatigue operation, and shortage of lubricant, which causes various faults in the shaft parts and the bearings of the rotating parts, such as friction, cracks, and eccentricity [18, 19]. Therefore, it is necessary to denoise and process the vibration signal collected by the sensor. To diagnose the fault of the rolling shaft of a rotating machine, it is necessary to first collect vibration signal, process signal noise reduction, extract fault characteristic signals, identify and classify fault states, and diagnose fault degrees [20, 21]. Figure 1 shows the diagnostic flow of rotating machinery equipment.

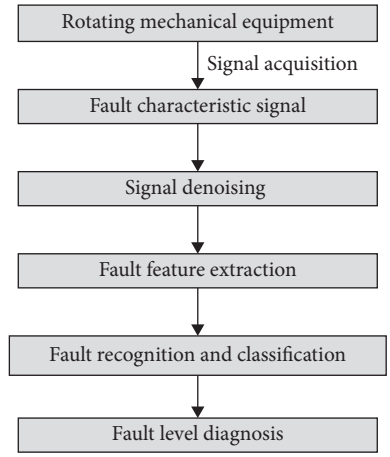

Figure 1: Flowchart of fault diagnosis of rotating machinery equipment.

2.2. Rotating Machinery Vibration Signal Processing Method. In the early stage of failure during engineering application, the weak rotating machinery vibration signal collected will be submerged by the background noise signal, so the core of feature extraction is to eliminate the background noise accurately.

2.2.1. Stochastic Resonance Theoretical Model. A bistable system of stochastic resonance is represented by the following equation:

$$\left\{\begin{array}{c} \dfrac{dx}{dt} = ax - bx^3 + A\cos\,\Omega t + \Gamma(t) a > 0, b > 0 \\ f(t) = ax - bx^3 \\ E[\Gamma(t)] = 0 \\ E[\Gamma(t)\Gamma(t)\imath] = 2D\delta\left(t - t'\right) \end{array}\right\}. \quad (1)$$

The above formula $A\cos\Omega t$ represents the external periodic driving force, a and b are both constants, x is the signal, A and O represent the amplitude and angular frequency of the external periodic driving force, $\Gamma(t)$ represent white noise, D represents noise intensity, E represents mean function, and $\delta(t - t\imath)$ represents shock function. If there is no external noise and driving force, that is, A and D are equal and zero, the potential well equation of the above equation is expressed as

$$V(t) = -\frac{a}{2}x^2 + \frac{b}{4}x^4, \quad (2)$$

where $V(t)$ is the potential well. The periodic signal passes through the system, and its signal is very weak, which makes it difficult to push the particles from one potential well to other potential wells. If a driving noise synchronized with the periodic force is actively added from the outside, the particles can pass over the potential well, and random resonance can be generated.

2.2.2. Chaos Particle Swarm Optimization Algorithm. We initialize the particle position and velocity based on chaos theory, let the standard particle swarm algorithm form a chaotic state after initialization, and make the initialization show the characteristics of regularity, diversity, and ergodicity. Logistic map is one of the most representative chaotic systems:

$$Z_{n+1} = \mu Z_n\left(1 - Z_n\right) n = 0, 1, 2, \ldots, \quad (3)$$

where μ represents the control variable. Assuming that the value of μ is 4 and the value range of Z_0 is (0, 1). Logistic is in a chaotic state. Based on the convenience, randomness, regularity, and other characteristics of chaotic variables, we initialize the random resonance position and initial speed and make them traverse differently, so as to improve the individual quality of particles and improve the search effect.

2.2.3. Variational Mode Decomposition (VMD) Algorithm. In this study, the variational mode decomposition (VMD) algorithm is used to solve the problem of rotating machinery vibration signal processing and the empirical mode decomposition (EMD) end effect problem. The VMD algorithm is used when decomposing and reconstructing the rotating machinery vibration signal, and the characteristic signal is reconstructed. We run the modal formation of the envelope spectrum analysis and then further extract the fault signal features. The VMD algorithm decomposes the $f(t)$ input signal into a series of intrinsic modal function u_{k} models of band-limited blocks; each u_{k} model surrounds w_k; the following is the calculation formula:

$$\min_{(u_k)(w_k)} \left\{ \sum \left\| \partial t \left[\left(\delta(t) + \frac{j}{\pi t} \right) * u_k(t) \right] e^{-jwk^t} \right\|_2^2 \right\}, \quad (4)$$

where $\{u_{\mathrm{k}}\} = \{u_1, u_2, ..., u_{\mathrm{k}}\}$ represents the entire model set and $\{w_k\} = \{w_1, w_2, \ldots, w_k\}$ represents the center frequency of the model set.

2.3. Fault State Identification of Rotating Machinery Based on High-Order Cumulants. Based on modern signal processing theory, high-order moments and high-order cumulants are obtained by derivation of characteristic functions, and the high-order cumulants are regarded as a kind of high-order statistics. Assuming that x represents a continuous random variable and $f(x)$ represents the probability density function, the calculation formula in the moment generating function $\Phi(w)$ is as follows:

$$\Phi(w) = \int_{-\infty}^{\infty} f(x) e^{\mathrm{j}\omega x} dx. \quad (5)$$

The moment generating function needs to calculate the k-order derivative of the moment generating function $\Phi(w)$. Assuming that the value of ω is 0, the calculation formula of the k-order moment m_{k} of the random variable x is as follows:

$$m_k = (-j)^k \frac{d^k \Phi(\omega)}{d\omega^k} \bigg|_{w=0} = (-j)^k \Phi^{(k)}(0). \quad (6)$$

The natural logarithm $\Phi(w)$ in the moment generating function is the cumulant generating function, and the calculation formula is as follows:

$$\Psi(\omega) = \mathrm{In}\Phi(\omega). \quad (7)$$

We calculate the k-order derivative of the cumulant generating function; assuming that the value of ω is 0, the k-order cumulant $\mathrm{C_{kx}}$ of the random variable x can be obtained based on the following formula:

$$C_{k\,c} = (-j)^k \frac{d^k \Psi(\omega)}{d\omega^k} \bigg|_{w=0} = (-j)^k \Psi^{(k)}(0). \quad (8)$$

Generally, cumulants exceeding the 3rd order is regarded as high-order cumulants.

2.4. Fault Diagnosis of Rotating Machinery Based on LMD Morphological Filtering. The local mean decomposition method belongs to the adaptive signal analysis method. It forms pure FM signal and envelope signal by separating any nonstationary signal $x(r)$. The following is the detailed decomposition process:

(1) Calculate the local extreme point envelope value a_i and average value m_{i} based on $x(t)$:

$$m_i = \frac{n_i + n_{i+1}}{2}, \qquad a_i = \frac{|n_i - n_{i+1}|}{2}. \quad (9)$$

(2) Connect a_{i} and m_i with a broken line to obtain the mean function $\mathrm{m11}(t)$ and the local envelope estimation function $\mathrm{a11}(t)$. Subtract $m_{11}(t)$ within $x(t)$:

$$h_{11}(t) = x(t) - m_{11}(t). \quad (10)$$

(3) After dividing $h_{11}(t)$ by $a_{11}(t)$, we can get $\mathrm{S_{11}}(t)$ FM signal:

$$S_{11}(t) = \frac{h_{11}(t)}{a_{11}(t)}. \quad (11)$$

(4) The value of $a_{12}(t)$ is 1. $\mathrm{S_{11}}(t)$ represents the standard FM signal; assuming $\mathrm{a12}(t) \neq 1$, $\mathrm{S_{11}}(t)$ represents the original data repetition process. When $S_{1\mathrm{n}}(t)$ is the standard FM signal, $\mathrm{a1_{(n+1)}}(t) = 1$.

(5) The envelope signal can be obtained by multiplying the local envelope estimation function:

$$a_1(t) = a_{11}(t) a_{12}(t) ... a_{1n}(t) = \Pi_{q=1}^{n} a_{1q}(t). \quad (12)$$

(6) The product of the first PF component is obtained by decomposition and the envelope signal $a_1(t)$ and $\mathrm{S_{1n}}(t)$. The first PF component obtained by decomposition is equal to the envelope signal.

(7) Decompose $x(t)$ into the sum of kth PF components and U_{k} as follows:

$$x(t) = \sum_{p=1}^{k} PF_p(t) = u_k(t). \quad (13)$$

3. Results

3.1. Build an Experimental Platform. One of the most used parts in various rotating machinery is rolling bearings. In

Table 1: Basic parameters of bearings selected for DDS experimental platform.

Bearing type	Number of balls	Ball diameter	Pitch diameter
6205-2RSJEMSKF	9	0.3206	1.524

Table 2: Fault characteristic frequency.

Fault type	Inner ring failure (Hz)	Outer ring failure (Hz)	Rolling element failure (Hz)
Eigenfrequency	23.16	36.54	55.2

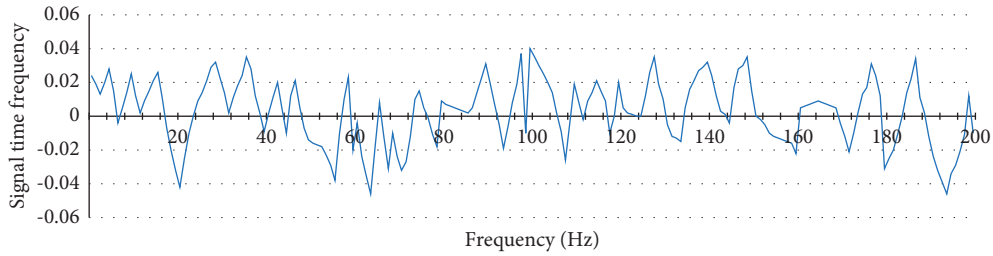

Figure 2: Time-frequency diagram of the acquired signal under the background of strong noise.

this study, a DDS power transmission fault diagnosis test bench is built, and the model is 6205-2RSJEMSKF bearing, 9 balls, and pitting damage is formed at the position of the bearing balls by electric sparks. Once the bearing has defects, the uniformly rotating rolling elements are affected by the defect to form a periodic shock signal, which is usually lower in frequency than the shock signal [22–24].

Rolling bearing is one of the most commonly used general components in all kinds of rotating machinery. This experimental platform is a comprehensive experimental platform for DDS power transmission fault diagnosis. The experimental bearing model is 200 Hz, and this frequency is the characteristic frequency of bearing faults. The data acquisition selects 16 channels, the bandwidth is 40 kHZ, the sampling frequency of the data collector is 100 kHz, and the collector is connected to the computer host by the USB interface [25, 26]. Table 1 is the basic parameters of the bearing. The motor speed is set to 600 r/min, and the sampling frequency is 1000 Hz. Forty percent of each group of data is collected, and 10 groups of data in four different modes are collected as training sample data, and then, 10 groups of data are collected, respectively. The group signal is regarded as the sample signal to be collected. Based on the fault characteristic frequency formula, three kinds of fault characteristic frequencies are obtained, and the specific results are listed in Table 2.

We substitute this parameter into the formula, and $\mathrm{COS}\alpha = 1$. The rotation frequency is 600r/min; the fault frequency can be obtained after calculation, which is listed in Table 2.

3.2. Noise Reduction Processing Results of Rotating Machinery Vibration Signals. In this study, accurate stochastic resonance parameters are obtained based on the chaotic particle swarm parameter optimization algorithm, and the fault sample signal is selected arbitrarily. Figure 2 is the spectrum diagram of the bearing rolling fault signal obtained through acquisition. It is difficult to distinguish accurately because the characteristic signal with strong noise is completely submerged.

Based on the chaotic particle swarm algorithm, $a_{\mathrm{best}} = 0.563$, $b_{\mathrm{best}} = 0.915$, and $h_{\mathrm{best}} = 0.194$ are obtained. At this time, the stochastic resonance effect of the bistable stochastic resonance system is the most ideal, so the signal at the fault frequency position has a significant increase. Then, the VMD parameters are optimized based on the mixed particle swarm algorithm, and the value of a is 1801, the value of k is 4, and the VMD is used to decompose the signal. After the adaptive chaotic particle swarm optimization stochastic resonance denoising process, the vibration signal VMD of the bearing can be decomposed to obtain the mode component of this certificate, of which the high-frequency part is significantly reduced.

Figure 3 is the result of the reconstruction of the measured signal, and the fault characteristic signal between the frequencies of 23 Hz and 24 Hz can be clearly viewed. Therefore, after denoising by stochastic resonance wavelet decomposition, the number of proof functions can be reduced so that the fault frequency increases and the high-frequency noise part decreases, thereby improving the analysis accuracy. Table 3 shows the vibration signals actually measured in a strong noise environment, so it is concluded that the processing effect of the noise reduction method used in this study is more ideal than the traditional VMD method.

3.3. Rotating Machinery Fault State Identification Results Based on High-Order Cumulants. Based on the high-level accumulation algorithm, this study selects 56 data points as one segment and selects the first ten segments of the four bearing state data as the training data and the last ten segments as the test data. In Figure 4, we draw four different

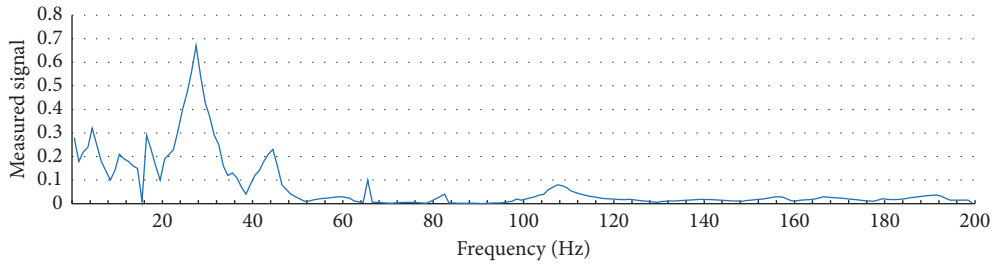

Figure 3: Measured signal reconstruction results.

Table 3: Comparison of the measured signal noise reduction effects of the two algorithms.

/	SA-VMD	VMD
SNR before processing	−23.71	−23.71
SNR after processing	−8.69	7.91

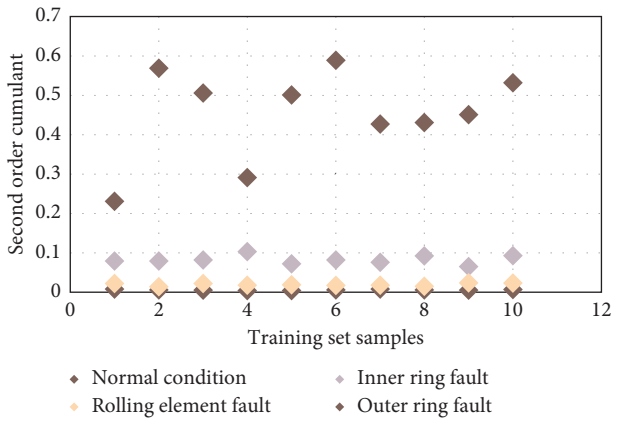

Figure 4: Second-order cumulant graph of bearing training samples.

states of the bearing and use different marks to indicate the second-order cumulative amount of the bearing state, as shown in Figure 4 [27–29].

According to the data in the figure, the normal state and the rolling fault state of the rear adjustment are similar, and the exact difference cannot be seen. We combine the second-order cumulants and fourth-order cumulants of the first ten training sample data to the feature vectors, accumulate them in high order, and then select the second-order and fourth-order cumulants in the ten test sample data as feature vectors to identify the vector state. Figure 5 displays the recognition results [30].

In Figure 5, 1 is the fault-free state, 2 is the inner ring fault, 3 is the rolling element fault, and 4 is the outer ring fault. According to the figure, only the eighth test sample among the forty test samples belongs to normal data, and its identification result is shown as a rolling element failure, and the state identification accuracy rate reaches 95%. Table 4 shows the classification and identification results of the predicted test set.

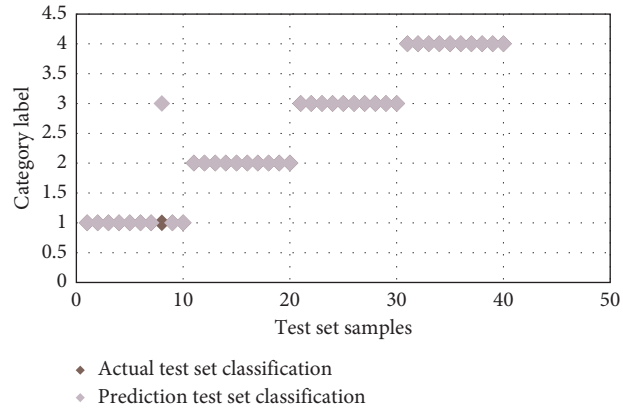

Figure 5: The high-order cumulative training and bearing identification results.

Table 4: Classification and recognition results of the prediction set.

Bearing status	Number of samples in the prediction set	Correct number of judgments	Recognition rate (%)
Normal situation	10	8	80
Inner ring failure	10	10	100
Rolling element failure	10	10	100
Outer ring failure	10	10	100
Total	40	38	95

There are certain differences in the vibration signals generated after the failure of the bearing roller, outer ring, and inner ring. Therefore, a number of indicators should be selected to calculate various fault vibration signals, and the number of indicators has dispersion. If the selected index is suitable, the obtained value has an ideal degree of discrimination for various fault signals. Since the accumulators have a good degree of discrimination for the fault signals of each bearing, various faults on the bearings can be accurately identified, and the fault identification effect is ideal.

3.4. Fault Diagnosis Results of Rotating Machinery Based on LMD Morphological Filtering. Most of the faults of rolling bearings are caused by local defects, and there are potential damages, which are difficult to detect in the early stage. Usually, the working environment of rolling bearings is

harsh, and the external environment is noisy. The vibration signal mainly includes other vibration responses of the machine system and the signal characteristics of the excitation mapping relationship, resulting in a low signal-to-noise ratio of the field vibration signal. The external environment will directly interfere with the bearing fault signal.

Local mean decomposition (LMD) is an adaptive time-frequency analysis method. It has strong mathematical morphological impact feature extraction ability and strong noise reduction ability. It can use morphological filtering in processing bearing vibration signals, which can fully reflect its own value. The original signal is processed by noise reduction to obtain a higher signal-to-noise ratio, and it can also extract the shock features in the fault. The following simulation signals are used to test the effect of extracting the signal-to-noise signal impulse characteristics by this method:

$$y(t) = x_1(t) + x_2(t) + nt, \tag{14}$$

where $x_1(t)$ represents a periodic exponential decay signal with a frequency of 16 Hz and n(t) represents a Gaussian white noise with a signal-to-noise ratio of −10 dB.

The bearing fault signal is decomposed based on LMD, and there is very little high-frequency fault data in the fourth PF component obtained through decomposition. Here, the first three IMF components are required and reconstructed. Then, the morphological filter is used to extract the characteristic frequency of the shock, and the adaptive morphological scale is optimized. The Hilbert envelope spectrum of the reconstructed signal is obtained after adaptive morphological filtering, which can accurately extract the 88 Hz shock signal and the frequency doubled component. The obtained result is similar to the fault frequency of the bearing inner ring, which means that there is a local peeling fault in the inner ring, which is in line with the actual situation and suppresses the noise spectral line, improving the signal-to-noise ratio. Through experiments, this extraction method can suppress white noise and various harmonic signals. The results after morphological filtering and LMD decomposition and extraction can avoid noise interference, and the analysis results after the harmonic order is higher than the third level have little interference to the spectrum with a higher signal-to-noise ratio.

4. Conclusion

(1) When studying the fault diagnosis of rotating machine based on adaptive vibration signal processing of safe environmental conditions, this study briefly introduces the basic process of fault diagnosis of rotating machine and points out that most of the faults of rotating machine come from bearing faults. By building the DDS dynamic rotation fault diagnosis test bench, the bearing model 6205-2RSJEMSKF is selected, and the common fault types are listed, namely, inner ring fault, outer ring fault, and rolling element fault. Based on the formula of fault characteristic frequency, different fault characteristic frequencies of three kinds of faults are calculated.

(2) This study describes in detail several methods commonly used in rotating machinery vibration signal processing, namely, random vibration theoretical model, chaotic particle swarm optimization algorithm, and variational mode decomposition (VMD) algorithm. Based on the chaotic particle swarm parameter optimization algorithm, the accurate stochastic resonance parameters are calculated. The results show that, after the stochastic resonance wavelet decomposition and noise reduction, the number of intrinsic functions can be reduced, the fault frequency can be increased, and the high-frequency noise can be reduced so that the characteristic signals can be accurately identified.

(3) This study identifies the fault state of rotating machinery based on high-order cumulants, trains the four states of the bearing, and compares the actual test set and the predicted test set with no faults, inner ring faults, rolling element faults, and outer ring faults. Results show that the rotating machinery fault is a rolling element fault and the averge recognition accuracy rate is as high as 95%. LMD morphological filtering is used to diagnose rotating machinery faults, and the bearing fault signal is decomposed based on the LMD algorithm.

Data Availability

The figures and tables used to support the findings of this study are included within the article.

Conflicts of Interest

The authors declare that they have no conflicts of interest.

References

[1] J. E. Ffowcs Williams and D. L. Hawkings, "Theory relating to the noise of rotating machinery," *Journal of Sound and Vibration*, vol. 10, no. 1, pp. 10–21, 1969.

[2] F. Lin, M. P. Schoen, and U. A. Korde, "Numerical investigation with rub-related vibration in rotating machinery," *Journal of Vibration and Control*, vol. 7, no. 6, pp. 833–848, 2001.

[3] L. Green, M. Shuttlesworth, and E. C. Buc, "Loss investigations involving heating element failures: fire, water, and personal injury," *Journal of Fire Sciences*, vol. 35, no. 3, pp. 195–206, 2017.

[4] S. Şeker, E. Ayaz, and E. Türkcan, "Elman's recurrent neural network applications to condition monitoring in nuclear power plant and rotating machinery," *Engineering Applications of Artificial Intelligence*, vol. 16, no. 7-8, pp. 647–656, 2003.

[5] C. M. Stoisser and S. Audebert, "A comprehensive theoretical, numerical and experimental approach for crack detection in power plant rotating machinery," *Mechanical Systems and Signal Processing*, vol. 22, no. 4, pp. 818–844, 2008.

[6] J. Lin and L. Qu, "Feature extraction based on Morlet wavelet and its application for mechanical fault diagnosis," *Journal of Sound and Vibration*, vol. 234, no. 1, pp. 135–148, 2000.

[7] H. Sun, Z. He, Y. Zi et al., "Multiwavelet transform and its applications in mechanical fault diagnosis–a review," *Mechanical Systems and Signal Processing*, vol. 43, no. 1-2, pp. 1–24, 2014.

[8] J. Li, X. Chen, and Z. He, "Multi-stable stochastic resonance and its application research on mechanical fault diagnosis," *Journal of Sound and Vibration*, vol. 332, no. 22, pp. 5999–6015, 2013.

[9] Y. Qin, S. Qin, and Y. Mao, "Research on iterated Hilbert transform and its application in mechanical fault diagnosis," *Mechanical Systems and Signal Processing*, vol. 22, no. 8, pp. 1967–1980, 2008.

[10] Y. Lei, F. Jia, J. Lin, S. Xing, and S. X. Ding, "An intelligent fault diagnosis method using unsupervised feature learning towards mechanical big data," *IEEE Transactions on Industrial Electronics*, vol. 63, no. 5, pp. 3137–3147, 2016.

[11] W. J. Wang, "Wavelet transform in vibration analysis for mechanical fault diagnosis," *Shock and Vibration*, vol. 3, no. 1, pp. 17–26, 1996.

[12] G. Chang, Z. Q. Zhang, and Y. Wang, "Review on mechanical fault diagnosis of high-voltage circuit breakers based on vibration diagnosis," *High Voltage Apparatus*, vol. 47, no. 8, pp. 85–90, 2011.

[13] Y. S. Fan and G. T. Zheng, "Research of high-resolution vibration signal detection technique and application to mechanical fault diagnosis," *Mechanical Systems and Signal Processing*, vol. 21, no. 2, pp. 678–687, 2007.

[14] H. L. Zhao, F. Wang, and X. G. Hu, "Application of wavelet packet energy spectrum in mechanical fault diagnosis of high voltage circuit breakers," *Power System Technology*, vol. 28, no. 6, pp. 46–48, 2004.

[15] Y. Lei, Z. He, and Y. Zi, "A new approach to intelligent fault diagnosis of rotating machinery," *Expert Systems with Applications*, vol. 35, no. 4, pp. 1593–1600, 2008.

[16] S. Dong, X. Xu, and J. Luo, "Mechanical fault diagnosis method based on LMD Shannon entropy and improved fuzzy C-means clustering," *International Journal of Acoustics and Vibration*, vol. 22, no. 2, pp. 211–217, 2017.

[17] Z. Dong, X. Tian, and J. Zeng, "Mechanical fault diagnosis based on LMD-approximate entropy and LSSVM," *TELKOMNIKA Indonesian Journal of Electrical Engineering*, vol. 11, no. 2, pp. 803–808, 2013.

[18] M. A. Kester, S. D. Cook, A. F. Harding, R. P. Rodriguez, and C. S. Pipkin, "An evaluation of the mechanical failure modalities of a rotating hinge knee prosthesis," *Clinical Orthopaedics and Related Research*, vol. 37, no. 228, pp. 156–163, 1988.

[19] D. Mba, R. H. Bannister, and G. E. Findlay, "Mechanical redesign of the rotating biological contactor," *Water Research*, vol. 33, no. 18, pp. 3679–3688, 1999.

[20] S. P. Das, D. P. Das, S. K. Behera, and B. K. Mishra, "Interpretation of mill vibration signal via wireless sensing," *Minerals Engineering*, vol. 24, no. 3-4, pp. 245–251, 2011.

[21] M. Z. A. Bhuiyan, J. Wu, G. Wang, Z. Chen, J. Chen, and T. Wang, "Quality-guaranteed event-sensitive data collection and monitoring in vibration sensor networks," *IEEE Transactions on Industrial Informatics*, vol. 13, no. 2, pp. 572–583, 2017.

[22] J. Bernstein, R. Miller, W. Kelley, and P. Ward, "Low-noise MEMS vibration sensor for geophysical applications," *Journal of microelectromechanical systems*, vol. 8, no. 4, pp. 433–438, 1999.

[23] C. Chen, F. Shen, J. Xu, and R. Yan, "Probabilistic latent semantic analysis-based gear fault diagnosis under variable working conditions," *IEEE Transactions on Instrumentation and Measurement*, vol. 69, no. 6, pp. 2845–2857, 2019.

[24] R. Yan, F. Shen, C. Sun, and X. Chen, "Knowledge transfer for rotary machine fault diagnosis," *IEEE Sensors Journal*, vol. 20, no. 15, pp. 8374–8393, 2019.

[25] Z. K. Abdul, A. K. Al-Talabani, and D. O. Ramadan, "A hybrid temporal feature for gear fault diagnosis using the long short term memory," *IEEE Sensors Journal*, vol. 20, no. 23, pp. 14444–14452, 2020.

[26] C.-H. Lin, C.-H. Wu, and P.-Z. Huang, "Grey clustering analysis for incipient fault diagnosis in oil-immersed transformers," *Expert Systems with Applications*, vol. 36, no. 2, pp. 1371–1379, 2009.

[27] Y. Zhang, Y. Qin, Z.-y. Xing, L.-m. Jia, and X.-q. Cheng, "Roller bearing safety region estimation and state identification based on LMD-PCA-LSSVM," *Measurement*, vol. 46, no. 3, pp. 1315–1324, 2013.

[28] I. I. E. Amarouayache, M. N. Saadi, N. Guersi, and N. Boutasseta, "Bearing fault diagnostics using EEMD processing and convolutional neural network methods," *International Journal of Advanced Manufacturing Technology*, vol. 107, no. 9, pp. 4077–4095, 2020.

[29] P. Shakya, M. S. Kulkarni, and A. K. Darpe, "A novel methodology for online detection of bearing health status for naturally progressing defect," *Journal of Sound and Vibration*, vol. 333, no. 21, pp. 5614–5629, 2014.

[30] G. F. Wang, Y. B. Li, and Z. G. Luo, "Fault classification of rolling bearing based on reconstructed phase space and Gaussian mixture model," *Journal of Sound and Vibration*, vol. 323, no. 3-5, pp. 1077–1089, 2009.